Astron. Astrophys. 273, 100–105 (1993)

ASTRONOMY
AND
ASTROPHYSICS

Spatial distribution of stellar mass in the Large Magellanic Cloud star clusters

A. Subramaniam, R. Sagar, and H.C. Bhatt

Indian Institute of Astrophysics,Bangalore 560 034, India

Received April 15, accepted December 17, 1992

Abstract. The stellar mass distributions have been studied in halo regions (radius ranging from $\sim$ 19 to 94 arcsec) of 5 young Large Magellanic Cloud star clusters. Effects of mass segregation have been observed in only NGC 1711. A comparison of cluster age with its relaxation time indicates that the observed mass segregation could have taken place at the time of star formation. Absence of mass segregation in most of the clusters may indicate that there is generally no spatial preference for the formation of massive stars. Most of the clusters have similar spatial density profiles which follow a power law with indices $\approx$ 3.5. This may indicate slow, but efficient process of star formation in the young star clusters of the Large Magellanic Cloud.

Key words: LMC – star clusters – mass segregation – star formation

1. Introduction

A study of the spatial distribution of stellar mass in young (age $\leq$ 100 Myr) star clusters can throw light on initial star formation processes because the time required for two-body encounter processes to obliterate most signatures of their initial states is $\sim$ 1 Gyr which is much larger than their ages. Such studies have been carried out in many young star clusters of our galaxy. A number of them show mass segregation in the form of preferential concentration of more massive stars in the central regions. This phenomenon can be understood easily in terms of dynamical relaxation of a star cluster, which leads to equipartition of kinetic energy in clusters members, with the result that low-mass stars occupy a larger volume than the massive stars. However, a recent study by Sagar et al. (1988) indicates that the observed mass segregation in extremely young open clusters (age $\leq$ 5 Myr) might have taken place at the time of star formation, while in open clusters older than some million years, it might have been due to a combination of both initial star formation conditions and dynamical evolutionary processes. It would be interesting to study the spatial distribution of stellar mass in the Magellanic Cloud (MC) star clusters because the evolutionary history of the MCs has been presumably very different from that of our galaxy (cf. Westerlund 1990; van den Bergh 1991 and references therein), and hence we expect the star clusters in the MCs to be different in many ways from the galactic clusters. In this paper we analyse the spatial distribution of stellar mass in 5 young (age $\leq$ 100 Myr) Large Magellanic Cloud (LMC) star clusters, namely NGC 1711, 2004, 2100, 2164, & 2214.

Elson et al. (1987) have studied the radial density distributions for 10 rich young LMC star clusters as a function of limiting magnitude ($\equiv$ mass) using star counts from photographic plates and found no indication of mass segregation except possibly for NGC 1866. Out of these ten, three clusters (NGC 2004, 2164 & 2214) are in common with the present work. In comparison with photographic plates, CCD images have several well-known advantages. A comparison of recent CCD data with older photographic ones indicates that photographic data may not only have systematically larger errors specially near the plate limit (cf. Hesser 1986; Sagar et al. 1991 hereafter Paper 1); but they may also affect the star counts (Hesser 1986; Richtler & de Boer 1989). Also in the case of CCD images, data incompleteness factor can be estimated more reliably by using the technique of artificially added stars (Sagar & Richtler 1991 hereafter Paper 2). Consequently, relatively more reliable results are expected by the use of CCD data.

The observational data used in the present analysis are described in the next section, the treatment of data incompleteness and field star contamination are described in Sects. 3 and 4 respectively. Spatial distribution of stellar masses, dynamical stage of the clusters and conclusions follow in the remaining sections.

2. Observational data

The data used in this study are taken from Paper 1. They are in the B and V photometric passbands for over 8,960 stars reaching down to V $\sim$ 21 mag. The data were obtained at the f/8.5 Cassegrain focus of the 1.54 m Danish telescope at the European Southern Observatory, La Silla, Chile using a RCA

Send offprint requests to: A. Subramaniam

Table 1. The core radius (R_c) and the stellar surface density (ρ) for clusters under study. The values of R_c are taken from Elson (1991). Errors in the density values are standard deviation.

Cluster	R_c	Radius range	$\rho(arcmin^{-2})$ in the V magnitude bins				
	($''$)	($'$)	≤ 15	15 – 17	17 – 18	18 – 19	19 – 20
NGC 1711	6.0	0.31 – 0.47	13.0±5.9	33.5±11.1	60.1±16.2	106.1±24.4	69.4±24.6
		0.47 – 0.63		28.2± 8.2	48.0±11.6	64.1±14.9	111.0±24.1
		0.63 – 0.82	2.4±1.6	9.7± 3.8	29.7± 6.8	39.8± 8.9	99.0±14.9
		0.82 – 1.02	1.8±1.3	7.9± 3.0	4.1± 2.7	30.6± 6.9	33.0± 9.1
		1.02 – 1.25		3.6± 1.9	7.7± 2.9	12.4± 4.1	30.2± 7.9
		1.25 – 1.57		0.7± 1.1	3.7± 1.9	9.5± 3.1	17.1± 5.2
NGC 2004	4.5	0.31 – 0.47	25.6±8.6	102.3±21.9	86.5±23.0	209.0±40.5	240.0±46.4
		0.47 – 0.63	5.2±3.3	44.6±11.1	37.0±12.1	82.5±19.4	106.2±24.1
		0.63 – 0.82	6.4±2.8	23.4± 6.0	22.8± 7.5	44.4±10.8	52.0±13.6
		0.82 – 1.02	0.6±0.9	3.8± 2.6	6.9± 4.0	15.6± 6.1	35.6±10.1
		1.02 – 1.25	2.1±1.2	7.2± 2.5	8.6± 3.5	7.0± 3.9	19.2± 6.7
NGC 2100	6.7	0.31 – 0.47	13.0±5.1	77.7±23.2	47.8±20.5	37.4±20.5	
		0.47 – 0.63	11.1±4.6	17.1± 7.9	47.5±14.5	39.2±14.4	
		0.63 – 0.82	12.3±3.8	30.5± 7.5	19.8± 6.4	31.5± 8.6	
		0.82 – 1.02	0.9±0.9	15.0± 4.1	14.3± 4.3	21.4± 5.7	
		1.02 – 1.25	3.7±1.5	8.5± 2.4	13.4± 3.2	15.3± 3.7	
		1.25 – 1.57	1.1±0.8	3.7± 1.5	8.0± 2.2	5.1± 2.2	
NGC 2164	5.8	0.31 – 0.47	7.8±4.6	47.1±14.5	38.3±15.5	94.2±27.0	180.0±45.5
		0.47 – 0.63	3.7±2.7	19.0± 7.0	4.6± 4.3	43.3±13.0	79.1±19.9
		0.63 – 0.82	4.5±2.5	1.5± 3.9	24.6± 6.5	40.3± 8.8	45.0±10.3
		0.82 – 1.02	1.8±1.3	8.1± 2.8	10.1± 3.5	21.8± 5.4	36.4± 7.4
		1.02 – 1.25	0.7±0.7	5.5± 2.0	2.5± 2.5	9.8± 3.2	20.3± 4.7
		1.25 – 1.57	0.5±0.5	1.1± 0.8	1.5± 1.2	2.4± 1.8	7.6± 2.8
NGC 2214	8.5	0.31 – 0.47	15.6±6.6	21.9± 9.5	82.3±22.4	180.1±37.6	226.6±50.3
		0.47 – 0.63	3.7±2.7	10.7± 5.1	36.4±10.4	74.6±16.7	107.8±21.9
		0.63 – 0.82	1.1±1.1	6.9± 3.0	18.0± 5.3	37.2± 8.1	63.9±11.6
		0.82 – 1.02	0.9±0.9	5.9± 2.4	2.1± 1.7	21.5± 5.1	37.7± 7.3
		1.02 – 1.25	0.6±0.6	4.1± 1.7	3.8± 1.7	14.6± 3.4	26.5± 4.8
		1.25 – 1.57	0.5±0.5	1.3± 0.9	3.5± 1.5	3.8± 1.9	11.0± 3.1

CCD chip of the 320×512 pixel in size where one pixel corresponds to 0.47 arcsec. Other details of observations and data reductions are given in Paper 1.

3. Treatment of data incompleteness

The procedure used to quantify the data incompleteness in our photometry has been described in detail in Paper 2. Briefly, using the results of the artificial star add experiments performed on a data frame (see Table 2 in Paper 2), we derived the ratios of recovered to inserted stars in different magnitude bins in a defined spatial region which give directly the completeness factor, CF, for that region as a function of magnitude. As the value of CF becomes smaller with decreasing brightness and increasing stellar crowding, we have derived a monotonic relation between the value of CF and magnitude by drawing a smooth curve through the points by eye with an accuracy of ∼ 10 and ∼ 2 % for innermost and outermost regions respectively (cf. Fig. 2 in Paper 2). In this way we have been able to derive the completeness factors CF(B) and CF(V) for the stellar counts derived from B and V frames respectively. However, we require the completeness factor for the stellar counts derived from a V, (B−V) diagram. This can be derived from the individual values of CF(B) and CF(V) considering the fact that the geometrical configuration of stars in both V and B frames of a cluster or field region is exactly the same, only the magnitude distribution is slightly modified due to the range of colours of the stars. Therefore, the completeness factor CF(V, (B−V)) at a given magnitude in V, (B−V) diagram will be mainly controlled by that CF value of B and V where completeness is less, i.e., the value of CF (V_i, $(B-V)_i$) at point (V_i, $(B-V)_i$) cannot be larger than the smaller value of the pair (CF(V_i), CF(B_i)). Consequently, we have used

$$CF(V_i,(B-V)_i) = min(CF(V_i), CF(B_i))\,, \qquad (1)$$

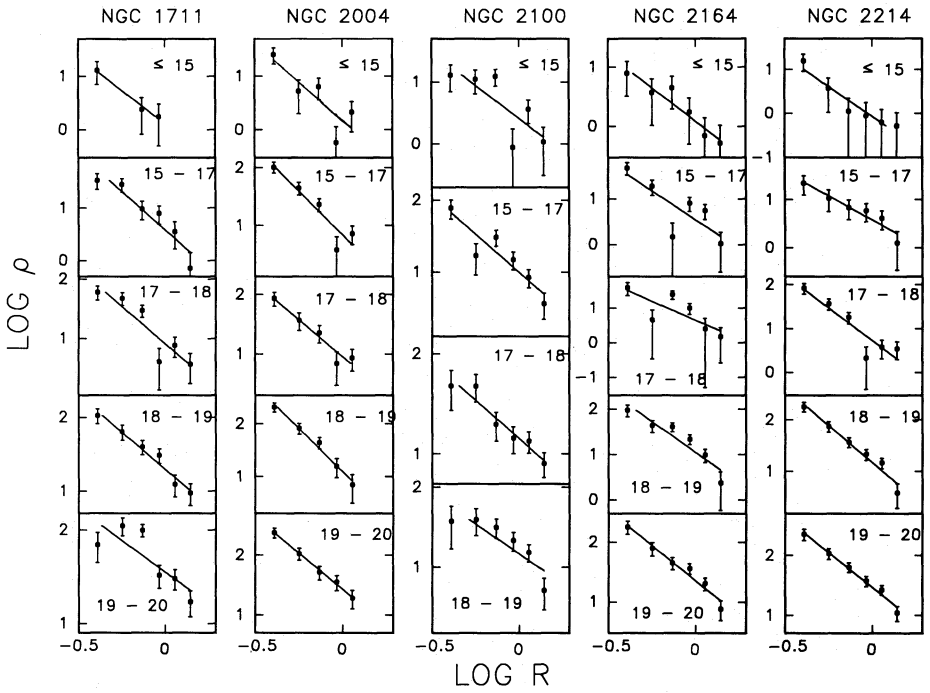

Fig. 1. Radial stellar surface density distribution in the LMC clusters, NGC 1711, 2004, 2100, 2164 and 2214. Continuous line is the least square fit to the observed points. Length of bar represents errors in density estimation at that point

for the data incompleteness correction in our further analysis. In this way the data incompleteness is little under corrected because this value of CF $(V_i, (B-V)_i)$ is the minimum correction. However, we believe that most likely it is close to reality.

4. Field star contamination

In order to evaluate the extent of field star contamination in the present analysis, we used the CMDs of the clusters and the field regions published in Paper 1. Field regions are generally located $\sim$ 4-10 arcmin away from the cluster centre. A comparison of this with the angular diameter of the programme clusters indicates that the probability of the presence of significant number of cluster members in the field regions is very low, while the probablity that the distribution of field stars in the cluster region can be represented very well by the stars of the imaged field region is very high. A comparison of the CMDs of the clusters and the field regions indicates that field star contamination is almost negligible for stars brighter than V $\sim$ 16 mag. So it is not statistically significant in the evolved parts of the cluster sequences since the clusters are younger than a few times 10^8 yr (cf. Paper 2) and consequently turn-off points in their CMDs are brighter than V $\sim$ 15 mag.

All clusters in their CMDs show a well defined cluster sequence from the main-sequence (MS) to the red supergiant phase as well as a concentration of stars at V $\sim$ 19.5 mag and (B−V) $\sim$ 0.9 mag (cf. Paper 1). These stars are intermediate-age core helium burning stars of the LMC field forming a "clump" in the CMDs and are not cluster members. We have therefore separated them from our further analysis by drawing a demarcation line between them and MS stars.

5. Radial stellar surface density

For the estimation of the radial surface density of stars in clusters, the cluster centre is first fixed. We have derived it iteratively by calculating average X and Y positions of stars within 150 pixels from an eye estimated centre, until it converged to a constant value. An error of a few arcsec is expected in locating the cluster centre. We have divided the stars into 5 V magnitude bins except in the case of NGC 2100, where only 4 bins could be made. The cluster area has been divided into a central (nucleus) and 6 annular regions, in such a way that each magnitude bin in a region generally contains statistically significant number of stars. The circular region with a radius of 40 pixels ($\equiv$ 4.7 pc) from the cluster centre is considered as the nucleus. The radius limits in pixels are 40 to 60, 60 to 80, 80 to 105, 105 to 130, 130 to 160 and 160 to 200 for annular region 1, 2, 3, 4, 5 and 6 respectively. At the distance of LMC, one pixel corresponds to $\sim$ 0.12 pc. For each magnitude bin, the number density of stars, ρ_i, in i^{th} zone has been evaluated as

$$\rho_i = \frac{N_i}{A_i}, \tag{2}$$

where N_i is the number of cluster stars and A_i is the area of the zone considered. To get the value of N_i, data incompleteness and field star contamination corrections have been applied to the observed number of stars, N_O, using the relation

$$N_i = \frac{N_O}{CF(V_i, (B-V)_i)} - NF, \tag{3}$$

where, CF$(V_i, (B-V)_i)$ is the completeness factor for the considered magnitude bin in the V, (B−V) diagram. The value of NF, the field star contamination, has been derived from the observed number of stars in the field region imaged for this pur-

Table 2. The reddening E(B−V) and the observed radial stellar surface density slope (γ) for different mass groups of the clusters under study. The standard deviation of the slope is denoted by σ_γ.

Cluster	E(B-V) (mag)	Mass Group	Mass range ($M_\odot$)	$\gamma \pm \sigma_\gamma$
NGC 1711	0.09	1	8.8 – 8.3	2.5 ± 0.46
		2	8.3 – 6.8	2.9 ± 0.51
		3	6.8 – 5.3	2.5 ± 0.54
		4	5.3 – 3.8	2.0 ± 0.20
		5	3.8 – 2.6	1.3 ± 0.45
NGC 2004	0.09	1	12.7 – 11.9	2.8 ± 1.10
		2	11.9 – 7.8	3.0 ± 0.70
		3	7.8 – 5.7	2.4 ± 0.37
		4	5.7 – 4.0	3.2 ± 0.23
		5	4.0 – 2.6	2.3 ± 0.10
NGC 2100	0.19	1	13.0 – 12.3	2.0 ± 0.87
		2	12.3 – 8.4	2.0 ± 0.44
		3	8.4 – 6.3	1.6 ± 0.25
		4	6.3 – 4.5	1.7 ± 0.54
NGC 2164	0.10	1	6.2 – 6.1	2.3 ± 0.45
		2	6.1 – 5.7	2.7 ± 0.44
		3	5.7 – 4.8	2.2 ± 0.88
		4	4.8 – 3.7	2.7 ± 0.49
		5	3.7 – 2.6	2.3 ± 0.24
NGC 2214	0.07	1	7.4 – 6.8	1.8 ± 0.28
		2	6.8 – 6.1	2.0 ± 0.29
		3	6.1 – 4.9	2.9 ± 0.64
		4	4.9 – 3.6	2.8 ± 0.26
		5	3.6 – 2.6	2.3 ± 0.14

pose, after applying the appropriate data incompleteness correction. The stellar surface density derived in this way for all the clusters is given in Table 1 along with the errors. In NGC 2004, statistically significant number of cluster members are not present in the 6th annular region. We have therefore not estimated the surface stellar density for this region. The log ρ versus log R plots for each magnitude bin of the clusters under discussion are given in Fig. 1. In NGC 2100, such plots can be made only for the four brightest V magnitude bins, because reliable estimate of ρ is not possible for the faintest magnitude bin. This is due to the fact that poor ($\sim$ 2 arcsec) seeing conditions during the observations have resulted in large data incompleteness in the stars where V is larger than 19 mag (cf. Paper 2). The value of ρ has not been estimated for nuclear regions of the clusters because the data incompleteness is very large there due to stellar crowding. As the nucleus is a circular region with a radius of $\sim$ 19 arcsec from the cluster centre, its size is much larger than the value of the core radius which is in the range of 4.5 – 8.5 arcsec for the clusters under study (cf. Table 1). Consequently, Fig. 1 shows the radial stellar surface density in those spatial regions which are well outside the core of the clusters.

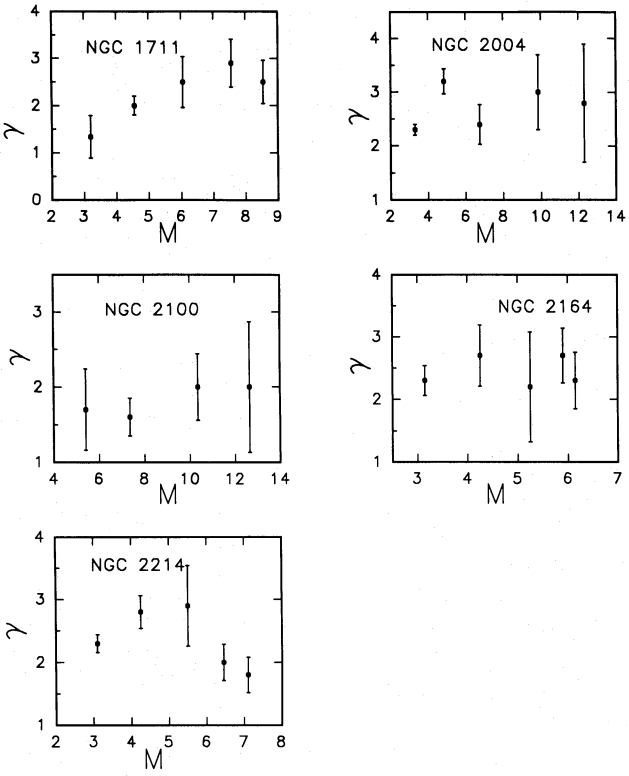

Fig. 2. The plot of γ versus average mass (in solar units) in the LMC clusters, NGC 1711, 2004, 2100, 2164 and 2214. Length of bar represents errors in γ

6. Spatial distribution of stellar masses

Elson et al. (1987) analysed aperture photometry and star counts in 10 LMC clusters and found that King models give poor fits to most of the surface brightness profiles at larger radii. Instead, the observed profiles could be represented by the simple formula

$$\rho(R) \propto \left(1 + \left(\frac{R}{constant}\right)^2\right)^{-\frac{\gamma}{2}}, \quad (4)$$

which reduces to

$$\log \rho(R) = a - \gamma \log R, \quad (5)$$

at larger radii, where a is a constant and γ is the power law index. In each observed profile, this relation is fitted and the coefficients are determined using the least squares solutions. The slope γ with its standard deviation σ_γ are given in Table 2. As the value of the correlation coefficient $| r |$ of the Eq. (5) is generally greater than 0.8, the assumption of the linear relation for the plots in Fig. 1 may be justified.

The mass ranges for the various magnitude bins of a cluster are calculated by fitting the theoretical stellar evolutionary isochrones given by Meader & Meynet (1991) to its V, (B−V) CMD and are listed in Table 2. We adopt a value of 18.6 mag for the true distance modulus of the LMC and assume the interstellar extinction in V as 3.1×E($B-V$) (cf. Paper 2). The E(B−V) values used for different clusters are given in Table 2.

The value of γ is plotted against the average mass of the group in Fig. 2. This shows that in a cluster the values of γ are almost the same for all mass groups except in the case of NGC 1711 where mass segregation effect is clearly visible. We assume normal error distribution for deriving the statistical significance level of the differences between the slopes of different mass groups in this cluster. The confidence levels in percentage for the difference in slopes are 96.4 between the mass groups 1 & 5 and 98.9 between the mass groups 2 & 5.

7. Dynamical stage of the clusters

Before deriving conclusions from the studies of the last section, it is necessary to know whether the location of stars in these clusters is representative of their initial distribution, resulting from the processes of star formation or not. At the time of formation, if the cluster had a uniform stellar surface density, then as the cluster evolves dynamically, the density changes and we would find the massive stars concentrated towards the center, as the low mass stars attained high velocity and moved away from the cluster center. Such a cluster is said to be dynamically relaxed. The dynamical relaxation time, T_E, is the time in which the individual stars exchange energies and their velocity distribution approaches a maxwellian equilibrium. The dynamical relaxation time, T_E, is given by

$$T_E = \frac{8.9 \times 10^5 \left(N R_h^3\right)^{\frac{1}{2}}}{\langle m \rangle^{0.5} \log(0.4N)} \quad (6)$$

where N is the number of cluster members, R_h is the radius containing half of the cluster mass and $\langle m \rangle$ is the average mass of cluster stars (cf. Spitzer & Hart 1971). We assume that R_h is equal to half of the cluster radius listed in Table 3. These angular values are converted into linear values by taking 1 arcsec equal to 0.25 pc at the distance of LMC. The average mass $\langle m \rangle$ and the value of N are based on the stars used in the present analysis. Finally, the dynamical relaxation time, T_E is calculated for all the clusters. In Table 3, column–3 contains the logarithmic values of the cluster age taken from Paper 2 and column–4 contains the logarithmic values of the T_E. The data considered for this work is limited to V $\sim$ 20 mag. The effect of considering stars fainter than this magnitude is to decrease the value of $\langle m \rangle$ and to increase the value of N. This will result in higher values of T_E. Hence the values of T_E given in Table 3 may be considered as the lower limit of T_E. A comparison of the age with the relaxation time indicates that the latter is always greater than the former indicating that two-body relaxation has not yet taken place in any one of these clusters.

8. Discussion and conclusions

The present analysis demonstrates that effects of mass segregation are present in the halo region of only one of the LMC star clusters studied here, namely, NGC 1711. Elson et al. (1987) also found that only one, namely NGC 1866, out of the 10 young LMC star clusters, showed evidence for mass segregation. The present day observed stellar distribution in the halo regions of the clusters younger than $\sim$ 100 Myr can be regarded as nearly the distribution of stars at the time of star formation, since they are not yet dynamically relaxed (cf. Table 3 and Elson et al. 1987) and the voilent relaxation and/or dissipation processes will modify only their core structure, if at all they are active. Hence the observed mass segregation in the halo regions of NGC 1711 and 1866 might have taken place at the time of star formation. Similar conclusions have been drawn by Larson (1982) and Sagar et al. (1988) from the studies of the spatial stellar distribution in some extremely young (age less than few Myrs) open star clusters of our galaxy. Absence of mass segregation observed in the halo regions of most of the young LMC star clusters may indicate that massive stars generally do not form with any spatial preference. From these discussions, one can conclude that star formation processes may not be the same in all star clusters of the LMC.

Surface brightness profiles of the rich young LMC star clusters have been studied by Elson et al. (1987) and Elson (1991). The former study is based on star counts derived from photographic plates while the latter one uses CCD images taken in B and V photometric passbands and includes all the clusters investigated by former. In order to compare the slopes of the surface

Table 3. Cluster age (T) and relaxation time (T_E). The cluster radii are taken from Shapley & Lindsay (1963).

Cluster	Radius (arcsec)	Log T	Log T_E
NGC 1711	103	7.5	8.4
NGC 2004	60	7.2	7.9
NGC 2100	68	7.2	7.9
NGC 2164	65	7.8	8.2
NGC 2214	93	7.8	8.4

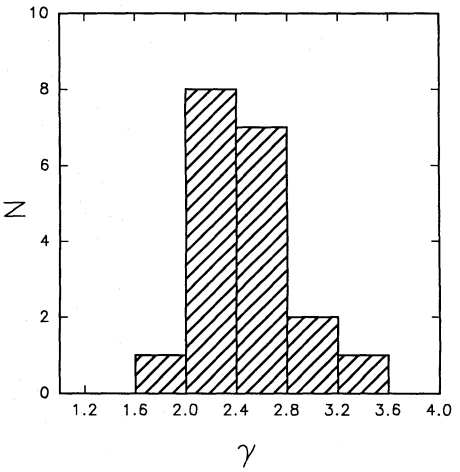

Fig. 3. The histogram of γ values for the star clusters in LMC

brightness profiles in the halo regions for the clusters under discussion, we studied the radial variation of stellar surface density in them. We plotted the radial stellar surface density in the 6 annular regions for a limiting magnitude of V $\equiv$ 20 against the cluster radii. The value of γ obtained from these plots are given in Table 4. Considering the uncertainties present in the γ values derived from different sources, one can conclude that the various estimates of γ for a cluster are in good agreement (see Table 4). From the surface brightness profiles given by Elson (1991), we estimated γ values for all the clusters. They are in the same range as found by Elson et al. (1987). Figure 3 shows their frequency distribution. The values of γ for most of the clusters are in the range 2.2 – 2.8 with a mean value of 2.5 $\pm$ 0.4. Present work thus confirms the earlier findings by Elson et al. (1987) that spatial density profiles for most of the young LMC star clusters fall off as power laws with indices $\gamma + 1 \approx$ 3.5 in the halo regions of the clusters.

Table 4. Comparison of the slope (γ) of radial stellar surface density for the clusters under study. A typical uncertainty in the γ values estimated from the surface brightness profiles given by Elson (1991) is $\sim$ 0.4.

Cluster	γ value obtained from		
	Elson et al. (1987)	Elson (1991)	Present work
NGC 1711		2.2	1.8 $\pm$ 0.2
NGC 2004	2.2 $\pm$ 0.2	2.0	2.4 $\pm$ 0.1
NGC 2100		2.2	1.5 $\pm$ 0.3
NGC 2164	2.8 $\pm$ 0.3	2.8	2.5 $\pm$ 0.3
NGC 2214	2.4 $\pm$ 0.2	2.3	2.4 $\pm$ 0.1

Crossing times for the rich young LMC star clusters are typically $\sim$ 6 Myr (Elson et al. 1987) and the time scale for forming stars and shedding unused material in such systems is $\lesssim$ 10 Myr (cf. Sagar 1987; Elson et al. 1987; Pandey et al. 1990 and references therein). These as well as the similarity of the observed stellar surface profiles in a number of rich and young star clusters located in different parts of the LMC may indicate slow but efficient star formation processes in them (Elson et al. 1987).

Acknowledgements. We thank the referee for valuable comments.

References

Elson, R.A.W. 1991, ApJS, 76,185
Elson, R.A.W., Fall, S.M., Freeman, K.C. 1987, ApJ, 323,54
Hesser, J.E. 1986, IAU Symp. No. 126, p. 61
Larson, R.B. 1982, MNRAS, 200, 159
Meader, A., Meynet, G. 1991, A&AS,89,451
Pandey, A.K., Mahra, H.S., Sagar, R. 1990, AJ,99,617
Richtler,T., de Boer, K.S. 1989, in recent developments of Magellanic Cloud Research, A European coll., K.S. de Boer, F. Spite, G. Stasinska Eds., published by Observatoire de Paris, p.45
Sagar, R. 1987, MNRAS, 228, 483
Sagar, R., Myakutin, V.I., Piskunov, A.E., Dluzhnevskaya, O.B. 1988, MNRAS, 234, 831
Sagar, R., Richtler, T. 1991, A&A, 250
Sagar, R., Richtler, T., & de Boer, K.S. 1991, A&AS, 90, 387
Shapley,H., Lindsay,E.M. 1963, IAJ, 6, 74
Spitzer, L.Jr., Hart, M.H. 1971, ApJ, 164, 399
van den Bergh, S. 1991, ApJ, 369, 1
Westerlund, B.E. 1990, A&AR, 2, 29

This article was processed by the author using Springer-Verlag LaTeX A&A style file version 3.